

94-365



СООБЩЕНИЯ  
ОБЪЕДИНЕННОГО  
ИНСТИТУТА  
ЯДЕРНЫХ  
ИССЛЕДОВАНИЙ  
ДУБНА

E14-94-365

A.Yu.Didyk

THE STRUCTURE OF ION TRACK  
IN SOLIDS PRODUCED BY IONS  
WITH HIGH LEVEL INELASTIC ENERGY LOSSES

1994

## 1. INTRODUCTION

Heavy ions of medium and intermediate energies are widely employed at studying the radiation effects in structural materials which are already in use and new promising ones for nuclear and being developed thermonuclear reactors [1]. Such ions have a variety of essential advantages in comparison with neutron sources. At the same time one should note that high specific ionizing energy losses exceeding 10 MeV/mm can make a certain contribution to the defect formation and can change the nature of accumulating radiation defects (see e.g. the work [2]). Therefore, the determination of the role of inelastic heavy ion energy losses is an important and actual scientific research problem. A considerable body of work is devoted to solving this problem [3,4].

One possible track formation can be the "thermal" peak and the coulomb "explosion", which are sufficiently well described in the literature [5].

One should note, that both these mechanisms are considered to fit the materials of dielectric-type where free electron density is low, due to this fact the time of electron excitations transferring to the lattice atoms is relatively high. That is, these models are assumed to be poorly suitable for metals and alloys.

Recently it has been predicted that heavy ion tracks with energies of MeV/amu have relatively small lateral size in diamond [6], actually in the range of about a few nanometers. A model of ion tracks in superhard semiconductors has been proposed in [7].

The production of ion tracks has been unambiguously established in many insulating materials by different methods [8,9], including direct observation with high resolution electron microscopy [10]. Ion tracks are specific defects of solids caused by high energy ion irradiation. The track formation mechanism and the parameters of the formed tracks are strongly controlled

by the intensity of electronic stopping power of the fast ions in solids and by the characteristic properties of the irradiated materials.

The theoretical estimations of track formation processes in metals were discussed in [11].

The amorphization of semiconductor single crystals irradiated by different heavy ions has been studied with the use of the back scattering technique [12,13]. The effect of low level amorphization of single crystals irradiated by heavy ions with a high level of inelastic energy losses has been obtained. The crater production under heavy ion irradiation on the surfaces of diamond single crystals [14] and stainless steel [15] has been established. The mechanism of inelastic sputtering of solids by ions has been described in ref. [16].

The purpose of this work is the phenomenological description of ion track formation in solids and the discussion of the criteria of material evaporation (sputtering) under heavy ion bombardment.

## 2. PHENOMENOLOGICAL MODEL

In the beginning we described the experimental data obtained after investigation of the samples irradiated by heavy ions.

The samples of boron doped diamond have been investigated by the scanning tunneling microscopy [14] before and after irradiation by the  $^{84}\text{Kr}$  ions. From the diameter distribution of the craters on the surface and theoretical proposal of the ion track sizes it has been concluded, that the craters with the diameter  $D_{\text{pit}} = 3 \text{ nm}$  are caused by single ions.

The surface of diamond irradiated by  $^{129}\text{Xe}$  and  $^{40}\text{Ar}$  ions has been investigated with the use of scanning electronic microscopy (SEM) [17]. The energies of these ions are 124 MeV and 25 MeV. Before the irradiation the diamond surface was a smooth one, but after the irradiation the regions of the surface have become

smooth and rough. In the case of  $^{129}\text{Xe}$  ions the diamond conserved the crystalline structure, but in the case of  $^{40}\text{Ar}$  ions the crystal has been totally amorphized [12]. Such differences may be connected with the evaporation of small diamond particles under the irradiation and then their subsequent condensation on the surface.

The surface of stainless steel irradiated by  $^{129}\text{Xe}$  ions at different temperatures and fluences has been investigated by SEM technique [15]. The needle structures have been observed. The total mass of needles on the surface is proportional to the ion fluence. From this fact it has been concluded that more than 90 atoms of the target have been evaporated and then condensed on the surface per one bombardment ion. The elemental composition of the needles is very different in comparison with the initial stainless steel composition. The main component in the needles is iron (more than 82 %, before the irradiation was 72 %).

The estimations of the evaporated volume sizes have been carried out and the diameter and depth of craters have been determined like this,  $D_{pit} \cong 16 \text{ A}$ ,  $X_{pit} \cong 16 \text{ A}$  after the simple calculations.

In the work [11] there has been discussed the process of formation as a result of ionizing and electron-electron relaxation of cylindrical region of the overheated electron gas the temperature of which is  $T_e$ , with the effective radius:

$$R_{e0} \cong \frac{I^2}{4\pi Z e^4 n} \quad (1)$$

where  $I$  - a mean ionization potential,  $Z$  - an atomic number,  $e$  - an electron charge,  $n$  - atom density of a target matter. The mean atom ionization potential can be approximately written as :

$$I \cong 13.5 Z \text{ eV.} \quad (2)$$

Substituting the equation (2) in (1) and taking into account that  $Z_{Fe} = 26$  (for stainless steel involving in the main iron (72%)) and  $Z_c = 6$  (for diamond), and  $n_{Fe} = 8.867 \times 10^{22} \text{ cm}^{-3}$  and  $n_c = 1.77 \times 10^{23} \text{ cm}^{-3}$ , one can find that the radius of the area of overheated electron gas has a value:

$$R_{e0}^{Fe} \cong 21 \text{ A}, R_{e0}^c \cong 2.4 \text{ A.} \quad (3)$$

The time of heat transferring from overheated electrons to the lattice  $\tau_{ei}$  equals:

$$\tau_{ei} = \frac{R_c^2}{\alpha_e} \quad (4)$$

here  $R_c$  is the radius of an energy track, and  $\alpha_e$  - the coefficient of electron gas thermal conductivity determined, mainly, by the length of electron-phonon collisions ( $\alpha_e = K_e / C_e$ ,  $C_e$  - electron specific heat).

After matching the electron and lattice temperatures the energy track takes the form of relatively slow thermal "spreading" which is characterized by a low value of temperature conductivity coefficient  $\alpha_T = K_e / C_i$  (here,  $K_e$  is the electron thermal conductivity, and  $C_i$  - specific lattice heat). A characteristic time of thermal spreading  $\tau_T$  is taken as a track lifetime in the work [11]:

$$\tau_T = \frac{R_c^2}{\alpha_T} \quad (5)$$

Then the track radius is determined by the equation:

$$R_c = \left( \frac{\gamma \alpha_T ((dE/dx)_{in=1})^{1/2}}{\beta (\pi \gamma)^{1/2}} \right)^{1/3} \quad (6)$$

where  $\gamma = C_e / T_e$ ,  $\beta$  - the coefficient of heat transferring

from electrons to the lattice. And the temperature in track is:

$$T_c = \frac{(dE/dx)_{in.e.l}}{\pi R_c^2 C_i \rho_i} \quad (7)$$

$\rho_i$  - matter density of the target.

For a number of metals typical track parameters, e.g. for Fe have been estimated [11]:

$$\begin{aligned} R_c &= 50 \text{ \AA}, & T_c &= 6000 \text{ K}, \\ \tau_{e,i} &= 6 \times 10^{-14} \text{ s}, & \tau_T &= 10^{-12} \text{ s}. \end{aligned} \quad (8)$$

The values of inelastic energy losses of heavy ions  $(dE/dx)_{in.e.l}$ , ions  $^{139}\text{Xe}$  ( $E = 124 \text{ M}\text{\AA}$ B)  $^{84}\text{Kr}$  ( $E = 210 \text{ M}\text{\AA}$ B) and  $^{40}\text{Ar}$  ( $25 \text{ M}\text{\AA}$ B) in stainless steel Cr18Ni10Ti and in diamond monocrystal are obtained by means of the TRIM-90 computer program. These results are given in Table 1.

$R_c^{1)}$  track radius is estimated according to results in the work [6],  $R_c^{2)}$  is taken from the work [11],  $R_c^{3)}$  is calculated using the equation (6) in terms of an estimate for  $R_c^{1)}$ .

Parameters for diamond and stainless steel used in equations (4) - (7) and in calculations made below are presented in Table 2.

Table 1

Ion	Energy MeV	Diamond			Stainless steel		
		$(dE/dx)_{in.e.l}$ MeV/mm	$R_p$ μm	$R_c$ Å	$(dE/dx)_{in.e.l}$ MeV/mm	$R_p$ μm	$R_c$ Å
Xe	124	25	6.34	50 <sup>1)</sup>	33.6	5.38	50 <sup>2)</sup>
Kr	210	19	3.9	47.6 <sup>3)</sup>	-	-	-
Ar	25	9	3.78	42 <sup>3)</sup>	-	-	-

Table 2

Stainless steel Cr18Ni10Ti		Diamond monocrystal	
$n_{Fe}$ = $8.867 \times 10^{22}$	$\text{cm}^{-3}$	$n_c$ = $1.77 \times 10^{23}$	$\text{cm}^{-3}$
$\rho_i$ = 8.05	$\text{g/cm}^3$	$\rho_i$ = 3.51	$\text{g/cm}^3$
$C_i$ = 0.65	$\text{J/g/K}$	$C_i$ = 1.92	$\text{J/g/K}$
$K_i$ = 27.8	$\text{W/m/K}$	$K_i$ = (5.5 - 30)	$\text{W/cm/K}$
$\alpha_i$ = $5.3 \times 10^{-2}$	$\text{cm}^2/\text{s}$	$\alpha_i$ = (0.81-4.44)	$\text{cm}^2/\text{s}$
$L_{evap}$ = $6.3 \times 10^3$	$\text{J/g}$	$L_{evap}$ = $6 \times 10^4$	$\text{J/g}$

Here  $C_i$  and  $\rho_i$  are the density and heat capacity of the materials,  $n$  is the atom density,  $K_i$  is the heat conductivity,  $\alpha_i$  is the temper conductivity,  $L_{evap}$  is the evaporation heat of the materials.  $R_p$  is the projective range of ions.

The parameters  $C_i$ ,  $K_i$  are determined for the temperatures higher than  $T > 1100 \text{ K}$  in table 2.

Let us assume the density of specific ionizing energy losses as:

$$\frac{d^3E}{dx dR d\phi} = \frac{1}{\pi R_c^2} (dE/dx)_{in.e.l} \exp(-R^2/R_c^2). \quad (9)$$

That is, we believe that radial distribution of heavy ion energy losses is in the form of the Gaussian distribution. Then, let us compute the energy of heavy ion which it loses in the volume of a material  $V$  in the form of cylinder with a height  $X_{evap}$  and radius  $R_{evap}$  using the equation (9):

$$\Delta E \cong (1 - \exp(-R_{evap}^2/R_c^2)) \int_0^{X_{evap}} (dE/dx)_{in.e.l} dx. \quad (10)$$

On the base of the values of specific energy losses and track radii given in Table 1 and also of parameters from Table 2 we have temperature distribution in track

from the depth along the ion range (Fig.1a) and in a radial direction (Fig.1b). In Fig.1a track radius dependence along ion range  $R_c(x)$ , obtained in view of calculated values  $(dE/dx)_{i_{n+1}}$  which in their turn depend on  $x$  (see equation (6)) is presented. In the same figure the temperature of diamond melting ( $T_{m+1} = 4300$  K) is shown by dashed line.

As seen from Fig.1a and 1b the temperature in track exceeds that one of diamond melting up to the depths  $X_T^{Kr}, X_T^{Xe}$  and radii  $R_T^{Kr}, X_T^{Xe}$ .

In the case of irradiating the stainless steel by  $^{129}\text{Xe}$  ions the track temperature on the surface of a target  $T_c \cong 12900$  K, that significantly exceeds the melting point  $T_{m+1} = 1673$  K.

Moreover, the lifetime of a track  $\tau_T$  many times exceeds the lifetime of heat transferring from electrons to the lattice  $\tau_{ei}$ :

$$\tau_T \gg \tau_{ei}, \quad (11)$$

therefore, the processes of material evaporation from the overheated area along the track may take place while the heat transferring from this area to the rest matrix (in times of temperature matching up to the temperature of a sample under irradiation  $T = 300$  K for diamond and  $T = 673 - 973$  K for stainless steel).

One should note that the temperature of irradiated sample as a thermodynamic parameter can be entered for the case when the processes are close to the equilibrium ones, that is, when the crystal lattice exists and the atomic binding is slightly disrupted. In question, when the temperature in track  $T > T_{m+1}$ , the meaning of the temperature itself should to be used with precaution.

Let us discuss more proper approach, in our opinion, in order to determine the observed effects.

In the processes of material evaporation, e.g. with the use of high-power electron beams there is taken the meaning of critical power density, with its increasing

the material actively evaporates. This value may be written using the following equation:

$$P_{cr} = \frac{\alpha_i L_{\text{evap}} X_{\text{evap}} \rho_i}{R_{\text{evap}}^2}, \quad (12)$$

here  $\alpha_i$  - the coefficient of thermal conductivity (see Table 2),  $L_{\text{evap}}$  - specific heat of evaporation,  $X_{\text{evap}}$  - the depth of evaporated layer,  $R_{\text{evap}}$  - its radius.

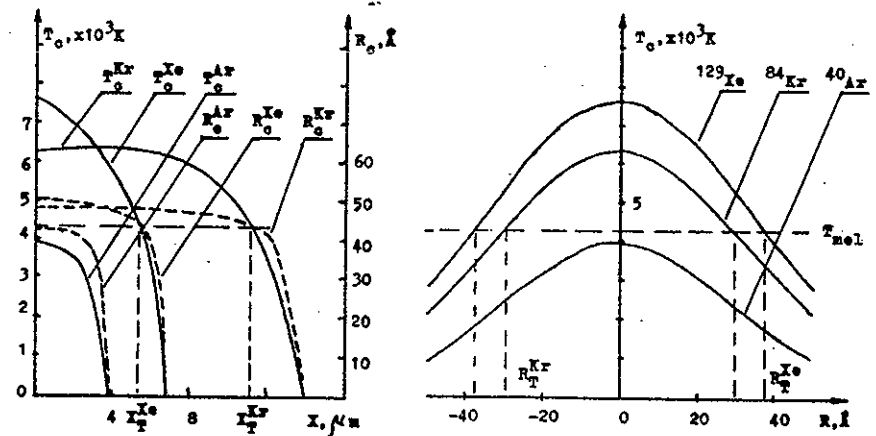


Fig.1. a) the dependencies of temperatures  $T_c(x)$  in heavy ion track  $^{40}\text{Ar}$ ,  $^{84}\text{Kr}$ ,  $^{129}\text{Xe}$  and track radii  $R_c(x)$  of the depth along the ion range,  
 b) the dependencies of radial temperatures  $T_c(R)$  in heavy ion track  $^{40}\text{Ar}$ ,  $^{84}\text{Kr}$ ,  $^{129}\text{Xe}$  of the distance from track axis.

Then the power density contributed by heavy ion can be written as:

$$P_{ion} = \frac{\Delta E}{\pi R_{\text{evap}}^2 t_{f1}}, \quad (13)$$

here  $t_{f1}$  - the time-of-flight of heavy ion of the layer

with the depth  $X_{\text{vap}}$ :

$$t_{r1} = \frac{X_{\text{vap}}}{(2E/M)^{1/2}}, \quad (14)$$

where, E and M - the energy and mass of a flying ion, respectively.

In the works [14,17] the diameter of craters on the surface of a synthetic diamond irradiated by  $^{84}\text{Kr}$  ions (E = 210 MeV) has been measured, it appeared to be equal to  $D_{\text{pit}} = 3$  nm. In the work [15] the estimates of diameter and crater depth, from which the target material evaporated (stainless steel) have been made and the values  $D_{\text{pit}} = 16$  Å,  $X_{\text{pit}} = 16$  Å have been obtained. In later calculations we assume that  $D_{\text{vap}} \cong D_{\text{pit}}$  and  $X_{\text{vap}} \cong X_{\text{pit}} \cong D_{\text{pit}}$ .

Comparing the value  $R_{\text{vap}}$  with the radius of overheated electron gas area (equation (3)) we see that  $R_{\text{vap}}^{\text{Fe}} < R_{\text{Fe}}^{\text{Fe}}$ , a  $R_{\text{vap}}^{\text{C}} > R_{\text{Fe}}^{\text{C}}$ .

Substituting  $R_{\text{vap}}$  and  $X_{\text{vap}}$  into equations (12) - (14) we find the values of critical power density  $P_{\text{cr}}$  and power density contributed by the ion  $P_{\text{ion}}$ . These values are given in Table 3.

Table 3

Ion	Energy MeV	Diamond		Stainless steel	
		$P_{\text{cr}}$	$P_{\text{ion}}$	$P_{\text{cr}}$	$P_{\text{ion}}$
$^{40}\text{Ar}$	25	$(0.23-1.25) \times 10^{13}$	$1.92 \times 10^{13}$	-	-
$^{84}\text{Kr}$	210	$(0.23-1.25) \times 10^{13}$	$8.88 \times 10^{13}$	-	-
$^{129}\text{Xe}$	124	$(0.23-1.25) \times 10^{13}$	$6.61 \times 10^{13}$	$6.69 \times 10^{10}$	$9.2 \times 10^{13}$

As seen from the comparison of data in Table 3, the power densities contributed by the ion exceed the values of critical evaporation power of a material ( $P_{\text{ion}} > P_{\text{cr}}$ ) for ions  $^{84}\text{Kr}$ ,  $^{129}\text{Xe}$  in diamond and for ions  $^{129}\text{Xe}$  in stainless steel. For ions  $^{40}\text{Ar}$  the peak value of critical

power matches that one by contributed ion. Therefore, the processes of material evaporation proceed highly efficiently in the case of the ions  $^{84}\text{Kr}$  and  $^{129}\text{Xe}$ . Moreover, for these ions the temperatures in tracks exceed the melting point in the region limited by the radius  $R_T$  and the depths  $X_T$  (see Fig.1).

For this reason in the cases of xenon and krypton ion irradiation the processes of carbon and stainless steel atom evaporation must be in the difference of argon ion irradiation because two conditions are realized:

$$P_{\text{Xe}} \gg P_{\text{cr}}, T_{\text{Xe}} > T_{\text{m.e.l}} \text{ and } P_{\text{Kr}} \gg P_{\text{cr}}, T_{\text{Kr}} > T_{\text{m.e.l}}. \quad (15)$$

The same criteria has been introduced for the description of evaporation processes in stainless steel irradiated by heavy ions [15]. The effects of inelastic sputtering of solids by ions have been described in ref. [16].

Let us discuss the structure of ion track taking into account the known experimental facts and relying upon their suppositions. In the works [12] and [13] one has determined the effect of retaining the long-range order in a number of semiconductor monocrystals for ion fluences, exceeding  $10^{16}$  ion/cm<sup>2</sup>, i.e., when due to elastic energy losses the complete amorphization of irradiated layer should take place. This phenomenon has occurred when inelastic energy losses of heavy ions have exceeded some threshold value.

In Fig.2 the structure of heavy ion track in terms of experimental facts (see the works [12]-[15], [17]) is shown. In the case when conditions (15) are met, on the surface of a sample at the ion input the crater is formed due to material evaporation with the following codensation of its part on the surface inhomogeneities. The crater has a diameter  $D_{\text{vap}}$  and the depth  $X_{\text{vap}}$ . In the volume of a track where the temperature exceeds the melting point (the region is as an ellipsoid of rotation with the radius  $R_T$  (X) and the length  $X_T$  (see Fig.1)),

from the bounding zone, where the temperature is close to that one of material recrystallization, to the track axis the processes of restoration of crystallic lattice structure take place (in Fig.2 these processes are shown by arrows). One should note that the central part of recrystallized area (track core) can have defects of growth, because the complete recrystallization in the ordered motion of recrystallization process from the boundary to the track axis is impossible. The region of a track limited by the radius  $R_c(x)$  and recrystallized area includes point defects (interstices and vacancies), the volume density of which decreases from recrystallized area to track boundary and increases as the depth grows up to projective range of heavy ion (in accordance with the increase of specific elastic energy losses of heavy ion).

It seems to us that such model provides an explanation not only for existence of craters on the surface, but a partial monocrystal amorphization under heavy ion irradiation with high specific energy losses as well (the level which with increasing the ion fluence practically is invariant (see, e.g. [12])).

At the same time it should be pointed out that the processes of evaporation - condensation and recrystallization can occur if characteristic periods of time of such processes  $\tau_{vap}$  and  $\tau_{rec}$  are lesser than the time of thermal track spreading  $\tau_T$  (see equation (5)), i.e.

$$\tau_{vap} < \tau_T, \quad \tau_{rec} < \tau_T. \quad (16)$$

In [18], on the base of analysis of annealing processes of semiconductor monocrystals at ion implantation and laser annealing it has been stated that at the boundary of overheated region - in track, due to high temperature the thermal conductivity coefficient and thermal conductivity are changed, respectively, that increases the time of existing the overheated region and decreases diffusion constants.

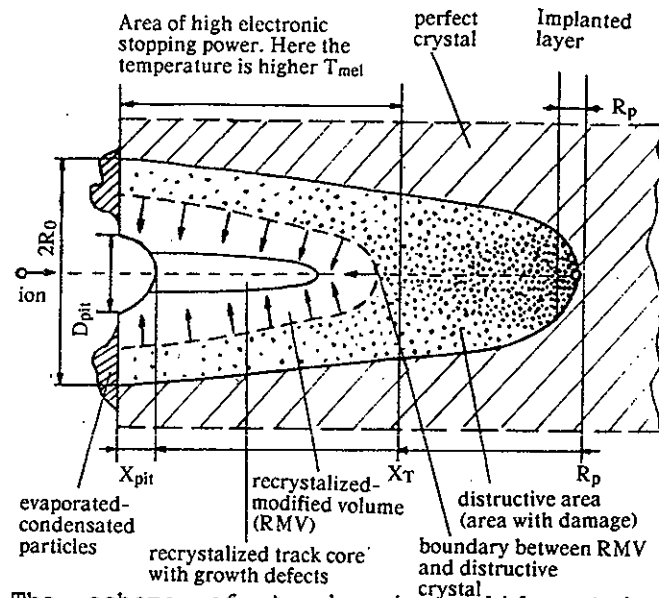


Fig.2. The scheme of tracks in solid matrix after irradiation by ions with energies over 1 MeV/amu, when the conditions (15) take a place.

## CONCLUSION

On the base of calculations one can conclude that if the conditions stated above are met (15) and (16) the processes of material evaporation with the following condensation on inhomogeneities of the surface can take place.

Moreover, to make more correct estimates in comparison with those performed in this work, one needs to carry out experimental investigations on direct measuring of crater sizes on the surface of irradiated materials induced by heavy ions with different inelastic energy losses. Such investigations are expected to continue in the future.

## REFERENCES

1. I.V.Altovskii. In: Itogi nauki i tekhniki. Metalovedenie i Termiceskaia obrabotka, v.21, p.3-52, 1987.

2. S.A.Karamian, Yu.Ts.Oganessian, V.N.Bugrov. Nucl.Instr. and.Meth., B43, p.153, 1989.
3. A.Dunlop and D.Lesueur. In: Materials Science Forum, V.97-99, p.553-577, 1992.
4. P.Legrand et al. In: Materials Science Forum, V.97-99, p.587-593, 1992.
5. R.L.Fleicher, P.B.Price, R.M.Walker. In.: Nuclear Tracks in Solids, University of California Press, Berkely (1975).
6. A.Yu.Didyk et al. JINR Commun. R14-86-411, Dubna (1986).
7. V.S.Varichenko et al. Sverhtverdye Materialy 1, p.3-8 (1989) (in Russian).
8. F.Thibaudau, J.Coustry, E.Balanzat, S.Bouffard. Phys. Rev.Lett. 67, p.1582-1585 (1991).
9. D.Albrecht, P.Armbruster, R.Spohr, M.Roth, K.Schaupert, H.Stuhrmann. Appl.Phys. A37, p.36-46 (1985).
10. J.M.Constantini, F.Ravel, F.Brisard, M.Caput, C.Cluzean. Nucl. Instrum. Meth. Phys. Res. B80/81, p.1249-1254 (1993).
11. A.A.Davydov, A.I.Kalinichenko. Voprosu Atomnoi Nauki i Tekniki 3[36], p.27-29 (1985) (In Russian).
12. S.A.Karamyan, Yu.Ts.Oganessian, V.N.Bugrov. Nucl.Instr. & Meth. B43, p.153 (1989).
13. A.Yu.Didyk, A.M.Zaitsev, S.A.Karamian. JINR Rapid Commun. No.4[37]-89, p.44-49 (1989).
14. V.S.Varichenko et al. In: Abstracts of 4<sup>th</sup> European Conference on Diamond, Diamond-like and Related Materials, Portugal, 1993.
15. A.Yu.Didyk. JINR Commun., R14-94-333, Dubna, p.13 (1994).
16. I.A.Baranov, Yu.V.Martynenko, S.O.Tsepelevich and Yu.N.Yavlinskii. Usp.Fiz.Nauk, v.156, p.477-511.
17. A.Yu.Didyk et al. In: The Book of Abstracts of 17<sup>th</sup> International Conference "Nuclear Tracks in Solids", Dubna, 1994, p.94.
18. J.Gyulai. Privat communication, 1994.

Received by Publishing Department  
on September 13, 1994.